

Competition of Spin Fluctuations and Phonons in Superconductivity of ZrZn_2

D. J. Singh and I. I. Mazin

Code 6390, Naval Research Laboratory, Washington, D.C. 20375

(Received 27 July 2001; published 19 April 2002)

It has long been suspected that spin fluctuations in ZrZn_2 may lead to a triplet superconductivity. We point out another possibility, an inhomogeneous singlet (Fulde-Ferrell) state. We calculated the electronic structure, as well as the zone center phonons and their coupling with electrons. We find that the exchange splitting is nonuniform and the Fermi surface exhibits substantial nesting. Both factors favor a Fulde-Ferrell state at parts of the Fermi surface. We find a substantial coupling of Zr rattling modes with electrons, which can provide the necessary pairing in the s -channel.

DOI: 10.1103/PhysRevLett.88.187004

PACS numbers: 74.20.Rp, 74.20.Mn, 74.25.Jb

The discovery of superconductivity in the ferromagnetic (FM) phase of ZrZn_2 [1] has revived interest in this compound. ZrZn_2 is a prototypical example of a weak itinerant (Stoner) ferromagnet. Very small magnetic moments (0.12 to $0.23\mu_B$) have been reported. These do not saturate even at fields up to 35 T, indicating the softness of the magnetic moment amplitude and suggesting the existence of soft longitudinal spin fluctuations. Already in the first report of ferromagnetism [2] it was pointed out that ZrZn_2 may be a FM superconductor, of the type discussed earlier by Ginzburg [3]. Later the idea of triplet spin-fluctuation induced superconductivity in FM ZrZn_2 was elaborated by Fay and Appel [4]. However, experimental searches for superconductivity in ZrZn_2 [5] were unsuccessful, till now. It is therefore tempting to identify ZrZn_2 as a triplet superconductor. This is supported by the fact that superconductivity seems to disappear with pressure at about the same point where the FM Curie temperature goes to zero. The low superconducting fraction does not allow accurate determination of the critical pressure for the superconducting transition to clearly show that it coincides with that for the magnetism. Thus one cannot fully exclude the possibility that the two types of orders are spatially separated. Still, it is likely that they do coexist, and if so, a key question is whether their interaction is constructive or destructive. A definite answer will require more study. However, before any theoretical speculations, one needs to get a detailed understanding of the electronic structure and its relation with superconductivity and magnetism. Here we present an accurate analysis of the paramagnetic and FM electronic structures and identify what seems to be the most interesting and relevant features of the band structure for superconductivity.

We find that the rigid band model is inappropriate for ZrZn_2 . The exchange splitting, $\Delta_{xc}(\mathbf{k})$, differs from band to band by more than a factor of 2. The Fermi surface shows substantial nesting features, suggesting that antiferromagnetic fluctuations may play a role in superconductivity. Even more importantly, nesting makes the superconducting pairing at some parts of the Fermi surface essentially 1D, in which case one can eliminate the pair-breaking effect of exchange splitting by constructing a spa-

tially inhomogeneous Fulde-Ferrell-Larkin-Ovchinnikov (FFLO) state [7], using the wave vector from the nesting of the spin-up and spin-down surfaces. Finally, we found that the rattling Zr modes are soft and couple strongly with electrons. So, while triplet superconductivity is an interesting possibility, the facts are compatible with a FFLO state of the s -wave symmetry as well.

ZrZn_2 occurs in a C15 structure; the Zr forms a diamond-type lattice, and the Zn forms a network of corner-sharing tetrahedra (i.e., a spinel structure without anions). An interesting aspect is the “overcoordination” of Zr: it has 16 nearest neighbors consisting of 12 Zn, forming a truncated tetrahedron (Fig. 1), at a distance (at $T = 50$ K [8]) 5.745 a.u., and 4 Zr at 6.001 a.u. The latter approximately corresponds to the bond length in Zr metal. Since the metallic radius of Zn is 16% smaller than that of Zr, Zr and Zn do not form strong bonds. On the other hand, Zr, unlike carbon, does not form highly directional bonds, so four Zr-Zr bonds in ZrZn_2 do not provide strong bonding either. This makes Zr “rattling” rather soft. At the same time, Zn has eight neighbors at a distance 4.9 a.u., noticeably less than in Zn metal (5.04–5.51 a.u.). So, Zn bond-stretching vibrations should be relatively hard.

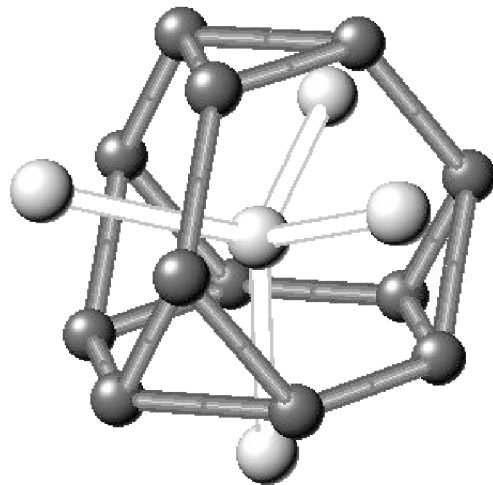


FIG. 1. Coordination of a Zr atom in ZrZn_2 .

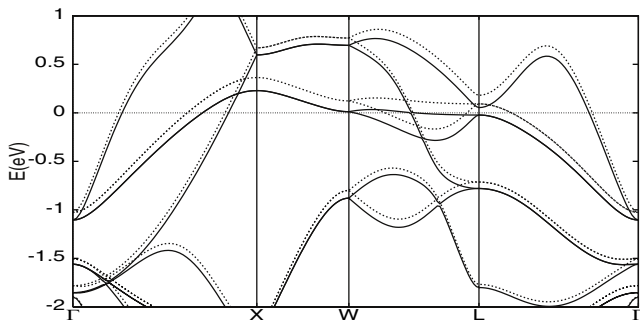


FIG. 2. LSDA band structure of ZrZn_2 . E_F is at 0. Solid (dashed) lines show majority (minority) bands corresponding to the magnetization of $0.2\mu_B$ f.u.⁻¹.

We calculated the band structure of paramagnetic and FM ZrZn_2 at the experimental lattice parameter of 13.858 a.u. [8]. The calculations were done in the local spin density approximation (LSDA) with the general potential linearized augmented plane wave method, including local orbitals [9]. The spin-polarized bands are shown in Fig. 2, and the Fermi surface in Fig. 3. Our calculations agree well with earlier ones (Refs. [10,11] and references therein). The basic characteristics of the nonmagnetic electronic structure are density of states at the Fermi level, $N(E_F) = 2.43$ states/eV spin f.u., Fermi velocity, $v_F = 2.5 \times 10^7$ cm/sec, plasma frequency, $\omega_{pl} = 4.0$ eV, Hall concentration $5 \times 10^{22} e \text{ cm}^{-3}$ [12]. The bands near the

Fermi level can be described in the first approximation as originating from the bonding combination of the t_{2g} Zr orbitals (the electronic sphere and the electronic rounded dodecahedron, both around the Γ point), and the bonding e_g orbitals (the “interconnected pancakes”). The tubular network Fermi surface is a hybridized combination of both types of states. However, such a view is oversimplified. Comparing the width of the d band of ZrZn_2 , and of the pure Zr sublattice (same calculations with Zn removed), we observe that the bandwidth, W , of the latter is about 30% smaller. Using the well-known tight binding formula, $W \propto \sqrt{\sum_i t_i^2}$ (where t_i is the hopping amplitude from the atom at origin to the i th neighbor), we see that $W_{\text{ZrZn}_2} \approx \sqrt{4t_{\text{Zr-Zr}}^2 + 12t_{\text{Zr-Zn}}^2}$, which gives a rough estimate of $t_{\text{Zr-Zn}} \sim 0.5t_{\text{Zr-Zr}}$, not surprising, given the smaller radius of Zn.

Although the effect of Zn on the total bandwidth is relatively small (cf. with the fcc Zr with the same Zr-Zr distance, which has a twice larger bandwidth, $W_{\text{Zr-fcc}} \approx \sqrt{12t_{\text{Zr-Zr}}^2}$ [13]), it is not negligible, and, interestingly, it is nonuniform over the Brillouin zone: the electron surface around the Γ point has more than 50% Zn character, while the other bands have nearly everywhere less than 20% (Fig. 3) [14]. This leads to a nonuniform exchange splitting $\Delta_{xc}(\mathbf{k})$ (Fig. 3). For instance, for the Fermi surface near the Γ point, the splitting of the Fermi surface, $\delta k_F \approx 0.017 \text{ \AA}^{-1}$, is smaller than $2\pi/\xi^{-1} \sim 0.022 \text{ \AA}^{-1}$, where

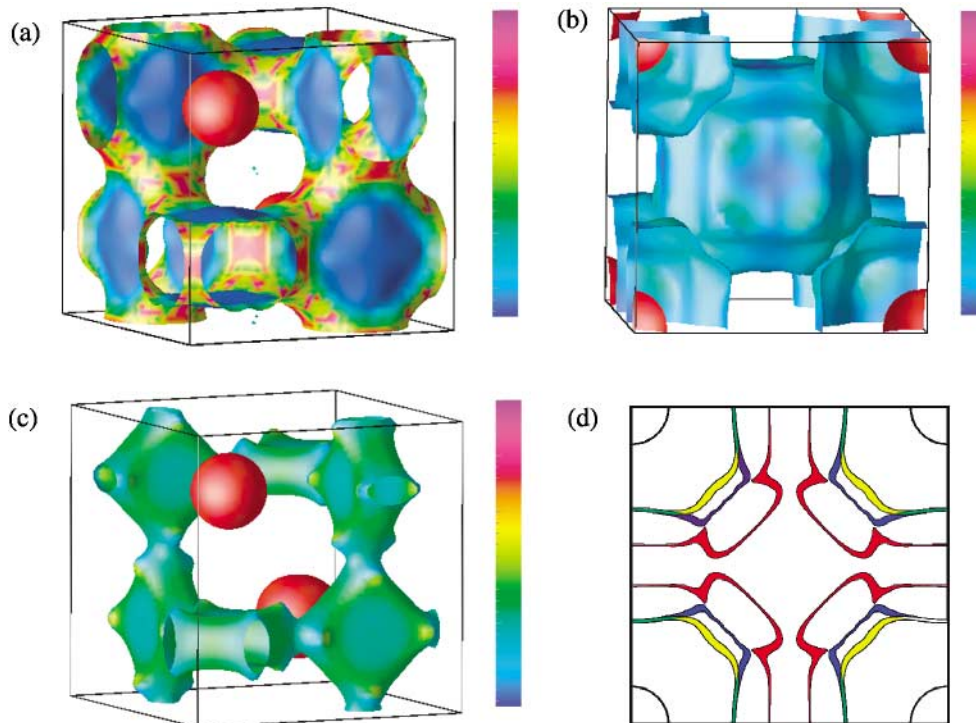


FIG. 3 (color). Fermi surface of ZrZn_2 . Panels (a), (b), and (c) show the nonmagnetic Fermi surfaces, colored by the relative percentage of Zn character. The color bar goes from 5% to 60%. The bands shown are (a) bands 1 and 2 (Γ points at the corners), (b) bands 1 and 3 (L points at the corners), and (c) bands 1 and 4 (Γ points at the corners). Panel (d) shows the Fermi surface 100 ($k_x = 0$) cross section. The widths of the lines correspond to actual exchange splitting for magnetization $M = 0.2\mu_B$.

$\xi \sim 290 \text{ \AA}$ is the superconducting coherence length [1]. This is favorable for the FFLO state, but, even more importantly, some of the Fermi surfaces exhibit strong nesting. If a piece of the spin-up Fermi surface nests, with some vector \mathbf{q} , a piece of the spin-down Fermi surface, then a spatially inhomogeneous FFLO state with the period $2\pi/q$ will have no exchange-splitting induced pair breaking at all. Not all electrons at the Fermi level form Cooper pairs in this case, but only those at the nesting parts of the Fermi surface.

The spin-polarized bands, used to produce panel (d) of Fig. 3, are shown in Fig. 2. These were calculated by fixing the total magnetization to be $0.2\mu_B \text{ f.u.}^{-1}$. Fully relaxed calculations converge to the value of $0.7\mu_B \text{ f.u.}^{-1}$, nearly 4 times larger than the accepted experimental value of $(0.17\text{--}0.20)\mu_B \text{ f.u.}^{-1}$. This is somewhat unexpected, for usually correlation effects, not completely accounted for in LSDA, tend to *increase* the tendency to magnetism. It may be that the actual samples are spatially inhomogeneous, with magnetic and nonmagnetic (and possibly superconducting) regions. Alternatively, the LSDA may overestimate the tendency to magnetism in this material, possibly due to quantum fluctuations associated with the critical point.

Near an itinerant ferromagnetic critical point, theory predicts a triplet superconductivity, with T_c first growing as one moves in either direction from the critical point, and then decaying as the spin fluctuations become weaker in either nonmagnetic or ferromagnetic phases. Such a behavior has been observed on the ferromagnetic side, for instance, in UGe_2 , and it was suggested that the difference between the longitudinal spin fluctuation spectra in the paramagnetic and ferromagnetic phases makes superconductivity much weaker and thus unobservable on the paramagnetic side [15]. So, a triplet state remains a plausible explanation for the superconductivity in ZrZn_2 . We want to call attention, however, to another possibility, namely, an FFLO inhomogeneous s -wave superconducting state. Both models can successfully explain the major experimental observations [1]: high sensitivity to sample purity (interband impurity scattering tends to make the order parameter the same for all bands, in which case the superconducting pairs feel a large exchange splitting of the more magnetic or less nested bands), absence of an observable specific heat jump (the Fermi surface sections with a large splitting may have vanishing gaps, which would greatly reduce the relative jump $\Delta C/C$), and disappearance of superconductivity near the FM critical point (because of the pair-breaking effect of spin fluctuations). A difference between the two models is that in the latter superconductivity not only is restored at pressures higher than critical (this is true for most models of the triplet superconductivity as well), but also, generically, T_c grows much faster on the paramagnetic side than on the ferromagnetic one. The high pressure data reported in Ref. [1] do not extend far enough beyond the critical point and do not give a definite

answer to whether superconductivity reappears at higher pressures. Unless the strongly interacting Zr rattling modes would harden substantially, and/or lose their coupling with electrons, under pressure, the FFLO scenario suggests superconductivity reentrance at a pressure high enough to suppress the spin fluctuations. We did check the pressure dependence of the T_{2g} mode (see Table I) and found that under a 3% volume compression it stiffens by 11%, while it softens by 6% under a 3% expansion.

A major question that arises now is, what would be the pairing interaction behind the assumed s -wave state? It needs to be sufficiently strong to make an FFLO state energetically competitive. To gain more insight, we performed calculations for the zone center optical phonons [16]. There are 15 such modes at six distinctive frequencies; four triple-degenerate T modes: T_{1u} (two), T_{2u} , and T_{2g} , one double-degenerate E_u mode, and one nondegenerate A_{1u} mode (Table I). The two softest modes correspond to a rattling motion of Zr inside the Zn cage, hence their softness and the small difference in their frequencies. As these two modes join at the zone boundary, one can see that they have little dispersion, as is common for rattling modes. The even (T_{2g}) mode is the only one that can couple with electrons at the Γ point, but as these two modes are essentially local vibrations, they presumably couple with about the same strength for general wave vectors, so the coupling constant computed for a T_{2g} mode should be a reasonable estimate for the coupling constants of all six rattling T_{2g} and T_{1u} phonons.

The coupling constant, defined as $\lambda_{\text{ep}} = 2 \sum_{\mathbf{k}\alpha} \times \delta(\epsilon_{\mathbf{k}\alpha} - E_F) (d\epsilon_{\mathbf{k}\alpha}/du)^2 / 2M\omega^2$, where $\sum_{\mathbf{k}\alpha} \delta(\epsilon_{\mathbf{k}\alpha} - E_F)$ is the density of states at the Fermi level per spin, M is the ionic mass, ω is the phonon frequency, and $(d\epsilon_{\mathbf{k}\alpha}/du)^2$, is $\lambda_{\text{ep}} = 0.115$. This mode is triple degenerate at Γ , so the total contribution to λ_{ep} from this mode is ≈ 0.35 . However, since we expect that all rattling modes of Zr would couple at a general point in the Brillouin zone with a similar strength, we estimate the total contribution from the six rattling modes to be ≈ 0.7 . Finally, the remaining 12 modes (especially the two rather soft E_u modes, which we expect to couple less with electrons) should bring a smaller, but finite contribution to the total λ_{ep} , so we take as a rough estimate $\lambda_{\text{ep}} \approx 1$. With a Coulomb pseudopotential $\mu^* = 0.1$, the McMillan formula yields $T_c \approx 10 \text{ K}$. This is a reasonable number since spin fluctuations should reduce T_c (and eventually eliminate superconductivity) in this scenario. This is also consistent with the

TABLE I. Zone center phonon modes in ZrZn_2 .

Mode	T_{2g}^a	T_{1u}^b	E_u^c	T_{1u}^d	A_{1u}^e	T_{2u}^c
Character	Zr	Mostly Zr	Zn	Mostly Zn	Zn	Zn
$\omega \text{ (cm}^{-1}\text{)}$	120	133	142	182	250	277

^aOut-of-phase Zr rattling; ^bin-phase Zr rattling; ^cZn breathing (the tetrahedra breathe out of phase with each other); ^dmixed mode; ^eZn breathing (all three tetrahedra breathe in phase).

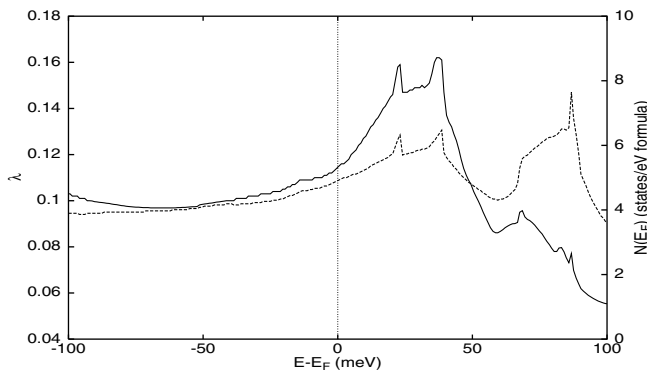


FIG. 4. Electron-phonon coupling constant, λ_{ep} , for one T_{2g} mode as a function of the Fermi level position. The solid line is λ_{ep} ; the dashed line is density of states.

transport coupling constant extracted from the linear part of the resistivity vs temperature dependence [17] of $ZrZn_2$ single crystals [18], $\lambda_{tr} = 1.4$. Assuming that $\lambda_{tr} \approx \lambda_{ep} + \lambda_{es}$, where λ_{es} characterizes coupling with spin fluctuations, we get $\lambda_{es} \approx 0.4$, and the modified McMillan formula then gives $T_c = (\omega_{ph}/1.2) \exp[-1.02(1 + \lambda_{ep} + \lambda_{es})/(\lambda_{ep} - \lambda_{es} - \tilde{\mu}^*)] \approx 0.3$ K. Here $\tilde{\mu}^* = \mu^*(1 + 0.62\lambda_{ep} + 0.62\lambda_{es})$. On the other hand, the specific heat coefficient of $47 \text{ mJ mol}^{-1} \text{ K}^{-2}$, reported in Ref. [1], corresponds to mass renormalization of 4.1, considerably larger than $(1 + \lambda_{ep} + \lambda_{es}) = 2.4$ [19]. This discrepancy may reflect the fact that thermodynamic and transport coupling constants need not be the same.

Another interesting observation is that the topology of the Fermi surface changes so sharply with chemical potential that the calculated coupling constant λ_{ep} is very sensitive to the exact position of the Fermi level in the band structure. In Fig. 4 we show its dependence on the Fermi level position. If the E_F were shifted by 20 meV, λ_{ep} would be 50% larger. This unusual sensitivity is only partially accounted for by the structure of the density of states (Fig. 4). Of course, the tendency to magnetism also strongly depends on the position of the Fermi level.

In conclusion, we report accurate calculations of the electronic structure and the zone center phonons in $ZrZn_2$ in both the paramagnetic and the ferromagnetic state. The recently observed superconductivity is compatible with any of the three scenarios: (i) sample inhomogeneity leading to separation of superconductivity and magnetism in real space, (ii) coexistence of ferromagnetism and inhomogeneous s -wave superconducting state (FFLO state), and (iii) triplet spin-fluctuation induced superconductivity. Further experiments may be able to distinguish between these three scenarios, since they predict three rather different thermodynamic behavior patterns: exponential BCS-like temperature dependencies, finite residual density of states, or a power law due to the gap nodes.

This work was supported by ONR and the ASC. We thank A. J. Millis, W. E. Pickett, and L. N. Bulaevsky for helpful discussions.

-
- [1] C. Pfleiderer, M. Uhlarz, S. M. Hayden, R. Vollmer, H. v. Löhneysen, N. R. Bernhoeft, and G. G. Lonzarich, *Nature (London)* **412**, 58 (2001).
 - [2] B. T. Matthias and R. M. Bozorth, *Phys. Rev.* **109**, 604 (1958).
 - [3] V. L. Ginzburg, *Sov. Phys. JETP* **4**, 153 (1957).
 - [4] D. Fay and J. Appel, *Phys. Rev. B* **22**, 3173 (1980).
 - [5] H. G. Cordes, K. Fischer, and F. Pobell, *Physica (Amsterdam)* **107B&C**, 531 (1981).
 - [6] T. F. Smith, J. A. Mydosh, and E. P. Wohlfarth, *Phys. Rev. Lett.* **27**, 1732 (1971).
 - [7] P. Fulde and R. A. Ferrell, *Phys. Rev.* **135**, A550 (1964); A. I. Larkin and Yu. N. Ovchinnikov, *Zh. Eksp. Teor. Fiz.* **47**, 1136 (1964) [*Sov. Phys. JETP* **20**, 762 (1965)].
 - [8] S. Ogawa, *Physica (Amsterdam)* **119B&C**, 68 (1983).
 - [9] D. Singh, *Phys. Rev. B* **43**, 6388 (1991).
 - [10] M. Huang, H. J. F. Jansen, and A. J. Freeman, *Phys. Rev. B* **37**, 3489 (1988).
 - [11] G. Santi, S. B. Dugdale, and T. Jarlborg, *Phys. Rev. Lett.* **87**, 247004 (2001).
 - [12] Note, however, that the Fermi surface topology is quite sensitive to the position of the Fermi level; shifting it by 40 meV in *either* direction makes the Hall coefficient change sign from electronlike to holelike. This suggests nontrivial temperature dependence of the Hall coefficient.
 - [13] Note that the hopping in the fcc lattice is $dd\sigma$, while in the diamond structure it is an average of $dd\sigma$ and $dd\pi$ hoppings, which gives an additional increase in the bandwidth, and that the diamond structure possesses a pseudogap due to the bonding-antibonding splitting of the two Zr, thus increasing the density of states at the Fermi level.
 - [14] This also can be seen in the shape of this band along the Γ -X line: in the nearest-neighbor Zr-Zr model, this band should be cosinusoidal, but a noticeable second harmonic component is clearly seen in Fig. 2. This is due to the Zn-assisted effective second neighbor hopping.
 - [15] T. R. Kirkpatrick, D. Belitz, T. Vojta, and R. Narayanan, *Phys. Rev. Lett.* **87**, 127003 (2001).
 - [16] Standard frozen-phonon techniques were used for the lattice dynamics calculations.
 - [17] L. W. M. Scheurs, H. M. Weijers, A. P. J. van Deursen, and A. R. de Vroomen, *Mater. Res. Bull.* **24**, 1141 (1989).
 - [18] The resistivity reported in Ref. [17] starts to deviate from the linear behavior already at $T \gtrsim 150$ K. This can be attributed to the saturation due to the proximity to the Ioffe-Regel localization. Indeed, the mean free path at $T = 150$ K, computed using the LSDA Fermi velocity, is only twice longer than the lattice parameter.
 - [19] This analysis is based on the assumption that λ_{es} is the same above and below the Curie temperature. This is partially justified by the fact that $\rho(T)$ does not show any anomaly at T_C [17].